

BBA 74238

## Temperature dependence of anion transport in the human red blood cell

M. Glibowicka, B. Winckler, N. Aranibar, M. Schuster, H. Hanssum,  
H. Rüterjans and H. Passow

*Max-Planck-Institut für Biophysik und Institut für biophysikalische Chemie der Universität Frankfurt,  
Frankfurt am Main (F.R.G.)*

(Received 11 April 1988)

(Revised manuscript received 10 August 1988)

**Key words:** Ion transport; Temperature dependence; Band 3 protein; (Human blood)

Arrhenius plots of chloride and bromide transport yield two regions with different activation energies ( $E_a$ ). Below 15 or 25 °C (for  $\text{Cl}^-$  and  $\text{Br}^-$ , respectively),  $E_a$  is about 32.5 kcal/mol; above these temperatures, about 22.5 kcal/mol (Brahm, J. (1977) *J. Gen. Physiol.* 70, 283–306). For the temperature dependence of  $\text{SO}_4^{2-}$  transport up to 37 °C, no such break could be observed. We were able to show that the temperature coefficient for the rate of  $\text{SO}_4^{2-}$  transport is higher than that for the rate of denaturation of the band 3 protein (as measured by NMR) or the destruction of the permeability barrier in the red cell membrane. It was possible, therefore, to extend the range of flux measurements up to 60 °C and to show that, even for the slowly permeating  $\text{SO}_4^{2-}$  in the Arrhenius plot, there appears a break, which is located somewhere between 30 and 37 °C and where  $E_a$  changes from 32.5 to 24.1 kcal/mol. At the break, the turnover number is approx. 6.9 ions/band 3 per s. Using  $^{35}\text{Cl}^-$ -NMR (Falke, Pace and Chan (1984) *J. Biol. Chem.* 259, 6472–6480), we also determined the temperature dependence of  $\text{Cl}^-$ -binding. We found no significant change over the entire range from 0 to 57 °C, regardless of whether the measurements were performed in the absence or presence of competing  $\text{SO}_4^{2-}$ . We conclude that the enthalpy changes associated with  $\text{Cl}^-$ - or  $\text{SO}_4^{2-}$ -binding are negligible as compared to the  $E_a$  values observed. It was possible, therefore, to calculate the thermodynamic parameters defined by transition-state theory for the transition of the anion-loaded transport protein to the activated state for  $\text{Cl}^-$ ,  $\text{Br}^-$  and  $\text{SO}_4^{2-}$  below and above the temperatures at which the breaks in the Arrhenius plots are seen. We found in both regions a high positive activation entropy, resulting in a low free enthalpy of activation. Thus the internal energy required for carrying the complex between anion and transport protein over the rate-limiting energy barrier is largely compensated for by an increase of randomness in the protein and/or its aqueous environment.

Abbreviations: DNDS, 4,4'-dinitrostilbene-2,2'-disulfonate;  
 $\text{H}_2\text{DIDS}$ , 4,4'-diisothiocyanodihydrostilbene-2,2'-disulfonate.

Correspondence: H. Passow, Max-Planck-Institut für Biophysik, Heinrich Hofmann Str. 7, Frankfurt am Main 71, D-6000 F.R.G.

### Introduction

The temperature dependence of the human band-3-protein-mediated anion exchange is unusually large. At low temperatures the activation energy is rather similar for  $\text{Cl}^-$ ,  $\text{Br}^-$ ,  $\text{SO}_4^{2-}$  and

phosphate, and amounts to about 30–35 kcal/mol. For  $\text{Cl}^-$  and  $\text{Br}^-$  the Arrhenius plots show a more or less pronounced break at 15 and 25°C, respectively, and above these temperatures the activation energy assumes a value of about 20 kcal/mol. No such break is observed for phosphate and sulfate up to 37°C (reviewed in Ref. 1).

Changes in activation energy suggest changes of the rate-limiting step of the reaction sequence that lead to ion translocation across the membrane. Brahm [2] has pointed out that at the temperatures at which the breaks in the Arrhenius plots of the halides occur, the turnover numbers of  $\text{Cl}^-$  and  $\text{Br}^-$  are about the same ( $4 \cdot 10^3$  ions/band 3 per s). He suggested, therefore, that this number is critical for the transition from one rate-limiting step to another.

In the present paper, an attempt was made to find out whether or not the break in the Arrhenius plot is confined to halides, or if such a break could also be observed for a divalent anion, such as sulfate, which penetrates about three orders of magnitude more slowly than the halides and hence cannot reach the critical turnover number. For this purpose it was necessary to extend the temperature range of the sulfate flux measurements to temperatures above 37°C. In view of the unusually large temperature dependence of band-3-mediated anion transport, we hoped that this increase of temperature would enhance the rate of anion transport much more than the rate of disintegration of the red cell membrane and of the heat denaturation of the band 3 protein. Our results confirm this expectation and show that it is possible to measure sulfate fluxes up to about 60°C before irreversible changes of the red cell membrane and of the anion transport protein become significant. It was found that the Arrhenius activation energy changed from about 32.5 kcal/mol below 37°C to 24.1 kcal/mol at temperatures above 37°C. Thus, deviations from a linear Arrhenius plot are not confined to the halides.

The flux measurements were supplemented by NMR-measurements of chloride binding to the band 3 protein, using the procedure described by Chan and co-workers [3]. These experiments served to verify the survival of the substrate-binding capacity of the transport protein at the elevated temperatures and showed that  $\text{Cl}^-$  binding and

$\text{Cl}^-/\text{SO}_4^{2-}$  competition for the binding site do not change much over the whole temperature range of 0–60°C. They extend previous observations on the change of half-saturation of  $\text{Cl}^-$  and  $\text{SO}_4^{2-}$  transport and indicate that enthalpy changes associated with substrate binding to the transport protein do not contribute significantly to the apparent activation energy of anion transport. Hence, the latter is essentially related to conformational transitions of the substrate loaded-transport protein. The results presented here and those of previous authors will be evaluated in terms of the theory of absolute reaction rates and further discussed in terms of ping-pong kinetics which are believed to apply to band-3-mediated anion exchange (reviewed in Refs. 1, 6 and 7).

## Materials and methods

### *Source of red cells*

Human blood (type O,  $\text{Rh}^+$ ) from healthy donors was obtained from the Red Cross Blood Bank, stored in acid-citrate-dextrose and used for up to 6 days after donation.

### *Preparation of red cell suspension*

The blood was centrifuged down in a Sigma centrifuge at 5000 rpm for 5 min and serum and leucocytes were aspirated. The red cells were then washed twice by resuspension in isotonic NaCl solution (166 mM NaCl) and centrifuged at 5000 rpm for 5 min. The packed cells were divided into two batches and resuspended at pH 7.4, at a hematocrit of 10% in a medium comprising 130 mM NaCl/1 mM  $\text{Na}_2\text{SO}_4$ /20 mM EDTA. To one batch of resuspended cells  $\text{H}_2\text{DIDS}$  was added to give a final concentration of 60  $\mu\text{M}$   $\text{H}_2\text{DIDS}$ . Both batches were incubated at 37°C for 60 min.

### *Preparation of resealed ghosts [4]*

Both batches of red cells were centrifuged at 5000 rpm for 5 min at 4°C and washed twice in ice-cold isotonic NaCl solution. A 50% suspension of the packed cells was hemolyzed (1 part cells to 40 parts hemolyzing medium) at 0°C for 5 min. The hemolyzing medium consisted of 4 mM  $\text{MgSO}_4$ /1.0 mM acetic acid and yielded a pH of about 6.1 in the final hemolysate. Subsequently, a concentrated, ice-cold EDTA solution was added

to give a final concentration of 20 mM EDTA. After 5 min the cells were centrifuged down in a Sorvall centrifuge at 17000 rpm at 0°C for 5 min and washed once in the buffer to be used for the flux measurements, i.e., either in chloride medium (130 mM NaCl/1 mM Na<sub>2</sub>SO<sub>4</sub>/20 mM EDTA (pH 6.5)) or in sulfate medium (108 mM Na<sub>2</sub>SO<sub>4</sub>/20 mM EDTA (pH 6.5)). The cells were then resuspended in their respective medium at a hematocrit of 20% and radioactive sulfate was added to give an activity of 2  $\mu$ Ci per ml suspension. The suspensions were kept on ice for 15 min and then resealed at 37°C for 45 min. The radioactive ghost suspensions were kept overnight at 8°C to be used in an experiment on the next day.

#### *Measurement of sulfate efflux in the temperature range 20–37°C*

To measure the sulfate efflux the suspensions were cooled on ice and the radioactively labeled ghosts were sedimented in a Sorvall centrifuge at 17000 rpm for 5 min at 0°C. They were then washed three times either in ice-cold chloride or sulfate medium. The efflux was initiated by mixing the packed ghosts with their respective flux media (i.e., either chloride or sulfate medium (pH 6.5)) which had been prewarmed to give, after mixing, the desired temperatures between 20 and 37°C. The flux medium for the H<sub>2</sub>DIDS-pre-treated ghosts also contained H<sub>2</sub>DIDS to give a final concentration of 60  $\mu$ M. The final hematocrit was 2%. 500- $\mu$ l aliquots from the suspensions were taken at different times and centrifuged down in a biofuge A table centrifuge at 13000 rpm for 1 min. From the supernatant, 250  $\mu$ l aliquots were mixed with 2.0 ml Quickscent 2000 and counted in a PRIAS Packard scintillation counter. To determine the total radioactivity ( $y_{\infty}$ ), 250  $\mu$ l of suspension were directly pipetted into scintillation vials and counted.

#### *Measurement of sulfate efflux in the temperature range 37–60°C [5]*

To measure the efflux at the more elevated temperatures, an inhibitor-stop technique was used [5]. The radioactively-labeled SO<sub>4</sub><sup>2-</sup> was washed away as described above. For the final centrifugation the packed ghosts were resuspended in 1 ml of the appropriate medium and the suspension

was transferred to 2-ml Eppendorf reaction vials. They were then centrifuged at 17000 rpm at 0°C for 12 min to achieve close packing of the ghosts. The supernatant was aspirated and the packed ghosts were kept on ice. The efflux was initiated by injection of 100  $\mu$ l of the packed ghosts into 5 ml of the respective media. A magnetic stirrer was used to achieve fast mixing of the ghosts with the buffer. The syringe was equipped with an adaptor for a 100  $\mu$ l micropipet. To ensure complete transfer of the ghosts, the syringe was filled prior to injection with 0.5 ml of the prewarmed flux medium. This served to flush the packed cells out of the micropipet during injection. 500  $\mu$ l aliquots of each suspension were sampled. The stop medium (at 0°C) contained the flux media (at pH 7.4), H<sub>2</sub>DIDS to give a final concentration of 75  $\mu$ M and flufenamate to give a final concentration of 120  $\mu$ M. The aliquots were centrifuged down as quickly as possible in a Biofuge A at 13000 rpm for 1 min and kept on ice, until 250  $\mu$ l of the supernatant could be transferred to scintillation vials for counting. To ensure the compatibility of the results obtained with and without the inhibitor-stop technique, the flux at 37°C was measured using both techniques. The results were indistinguishable. At 60°C, the flux was measured for 5 min, at 37°C for 40 min.

At temperatures above the physiological range, red blood cells may vesiculate and hemolyse. Visual inspection under the phase contrast microscope showed that after 5 min at 60°C, vesiculation is negligible. In the supernatant of a 1% cell suspension no hemoglobin can be detected by visual inspection. Systematic studies of thermal stability of human red blood cells by Gershfeld and Murayama showed less than 10% hemolysis after 5 h at 50°C [11].

#### *Evaluation of data*

The tracer efflux was measured at equilibrium, i.e., under conditions where the composition of the media inside and outside the ghosts was identical. Under these conditions, efflux of the radioactive isotope follows a single exponential. The rate constants for efflux were calculated by means of a non-linear least-squares curve-fitting program. The rate constants of the suspensions made from untreated ghosts were corrected for H<sub>2</sub>DIDS-insen-

sitive flux by subtraction of the rate constants measured with H<sub>2</sub>DIDS-pretreated ghosts. The activation energies  $E_A$  were calculated according to the Arrhenius equation

$$E_A = \frac{R(\ln k_1 - \ln k_2)}{(1/T_2) - (1/T_1)} \text{ kcal/deg per mol.}$$

### NMR measurements in the red cell ghosts

**Preparation of ghost suspension.** Ghosts were resealed and washed in the media indicated in the text and figure legends. They were then resuspended in media of the same composition in which they had been prepared. In these media, 16% of the H<sub>2</sub>O was replaced by <sup>2</sup>H<sub>2</sub>O. For the NMR measurements, samples of 2.5 ml were transferred to NMR tubes of 10 mm diameter. In most experiments, the cell suspensions (50% hematocrit) contained equal numbers of cells per ml. If not, corrections were made for differences of the cell counts. The cell counts were taken by means of a Coulter Counter.

NMR measurements were carried out on a Bruker AM270 NMR spectrometer with a multi-nuclear broadband probehead (<sup>35</sup>Cl resonance frequency = 26.47 MHz) with spin.

At zero time a sample with or without DNDS (final DNDS concentration 1 mM) was placed into a water-bath adjusted to a temperature 1 °C above the temperature inside the probehead and shaken for 1 minute. Then the NMR tube was transferred quickly into the temperature-adjusted probehead. Accumulation of pulses was started immediately after shimming.

At the higher temperatures (67, 60 and 53 °C), spectra were recorded every 1–2 min; at the lower temperatures every 2–3 min. For each spectrum between about 250 (at 67 °C) and 2500 (at 3 °C) pulses were accumulated. At the lower temperatures the shape of the <sup>35</sup>Cl peak was distorted by noise. For this reason, a larger number of pulses were accumulated.

Since the determination of Cl<sup>−</sup>-binding depends on a replacement of Cl<sup>−</sup> by DNDS, we assured ourselves that, in the absence of light at 60 °C, less than 5% of the *trans* isomer of DNDS is transformed into the *cis* isomer in 1 h.

### Evaluation of the spectra

Every spectrum was corrected with respect to phase and baseline (by eye) and then fitted to a Lorentz curve. This fit yielded the linewidth at half-height of the <sup>35</sup>Cl peak. The linewidths for samples without or with DNDS are designated Lb<sub>0</sub> or Lb<sub>+</sub>, respectively. The line broadening  $\Delta Lb = Lb_0 - Lb_+$  at a given temperature, as measured at constant protein concentration and under conditions of rapid exchange, is proportional to the amount of chloride bound to the DNDS-sensitive sites [3].

### Results

#### Survival of H<sub>2</sub>DIDS-inhibitable SO<sub>4</sub><sup>2−</sup> equilibrium exchange at 60 °C

To demonstrate that at 60 °C the red cell membrane remains an effective barrier against anion leakage and that, at this temperature, the band 3 protein continues to transport anions for a length of time sufficient to measure sulfate ion fluxes, the following control experiments were performed.

Red cell ghosts were equilibrated with <sup>35</sup>SO<sub>4</sub><sup>2−</sup> at 37 °C. To remove external <sup>35</sup>SO<sub>4</sub><sup>2−</sup>, they were washed at 0 °C in the same buffer in which the equilibration was performed. To initiate <sup>35</sup>SO<sub>4</sub><sup>2−</sup> efflux they were resuspended at 60 °C. Subsequently, samples were taken after suitable time intervals, mixed with a stopping solution and centrifuged. The radioactivity in the supernatant was counted and rate constants were calculated as described under Materials and Methods. The time-course of appearance of the radioactivity in the supernatant is represented in Fig. 1. It follows a single exponential. When the medium contained 60 μM H<sub>2</sub>DIDS, the <sup>35</sup>SO<sub>4</sub><sup>2−</sup> efflux was inhibited by at least 90%. This indicates that most of the sulfate flux measured at 60 °C is H<sub>2</sub>DIDS-sensitive and thus retains the most characteristic feature of band-3-mediated anion transport.

Additional experiments were performed to obtain some information on the time of survival of the band-3-mediated anion transport and of the permeability barrier of the ghosts. Suspensions of red cell ghosts were incubated at 37 °C with <sup>35</sup>SO<sub>4</sub><sup>2−</sup> until the radioactivity was equally distributed between ghosts and medium. The suspension was then transferred to 60 °C. After various lengths

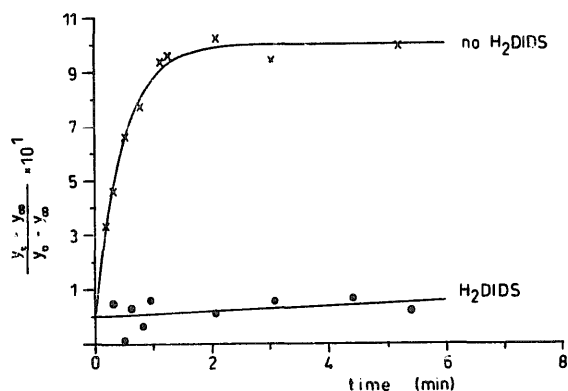


Fig. 1. Effect of  $\text{H}_2\text{DIDS}$  on sulfate equilibrium exchange at  $60^\circ\text{C}$ . Ordinate: fractional progress of the  $^{35}\text{SO}_4^{2-}$  efflux from resealed ghosts at  $60^\circ\text{C}$  in chloride medium (pH 6.5). The curve designated  $\text{H}_2\text{DIDS}$  refers to ghosts made from  $\text{H}_2\text{DIDS}$ -treated red cells (see Materials and Methods).  $^{35}\text{SO}_4^{2-}$  release from these ghosts was measured in chloride medium containing  $60\ \mu\text{M}$   $\text{H}_2\text{DIDS}$ .  $y_t$  = cpm at time  $t$ .  $y_\infty$  = cpm at equilibrium.  $y_0$  = cpm at time zero. The plotted curves represent non-linear least-squares computer fits of a single exponential to the data.

of time, samples were withdrawn, cooled to  $0^\circ\text{C}$ , and washed at that temperature in  $^{35}\text{SO}_4^{2-}$ -free medium to remove extracellular radioactivity and the intracellular radioactivity of leaky ghosts. The packed ghosts were then resuspended in  $^{35}\text{SO}_4^{2-}$ -free medium at  $37^\circ\text{C}$  and sulfate efflux was mea-

sured. From these measurements one obtains two pieces of information. (1) The total amount of radioactivity left in the red cell ghosts after incubation at  $60^\circ\text{C}$  for a given length of time. This is a measure of the fraction of ghosts in which the permeability barrier remained intact. (2) The rate constant of  $^{35}\text{SO}_4^{2-}$  efflux from the ghosts with surviving permeability barrier.

Fig. 2 and Table I show that the rate constants of  $^{35}\text{SO}_4^{2-}$  efflux, as measured at  $37^\circ\text{C}$ , do not change significantly up to about 15 min of preincubation at  $60^\circ\text{C}$ . This applies regardless of whether the efflux at  $37^\circ\text{C}$  was measured in the absence or presence of  $\text{H}_2\text{DIDS}$ . The percentage of radiosulfate retained by the ghosts after various lengths of exposure to  $60^\circ\text{C}$  changes with time, indicating that the fraction of leaky ghosts increases. This increase begins immediately after commencing the incubation at  $60^\circ\text{C}$  and amounts to about 1.5% per min. Interestingly enough, the membranes survive much better when the incubation at  $60^\circ\text{C}$  takes place after the binding of  $\text{H}_2\text{DIDS}$  to the band 3 protein (Table I).

In summary, the results described demonstrate that at  $60^\circ\text{C}$ , red cell membranes become leaky for sulfate, but the  $\text{H}_2\text{DIDS}$ -sensitive sulfate transport can be determined before this increased

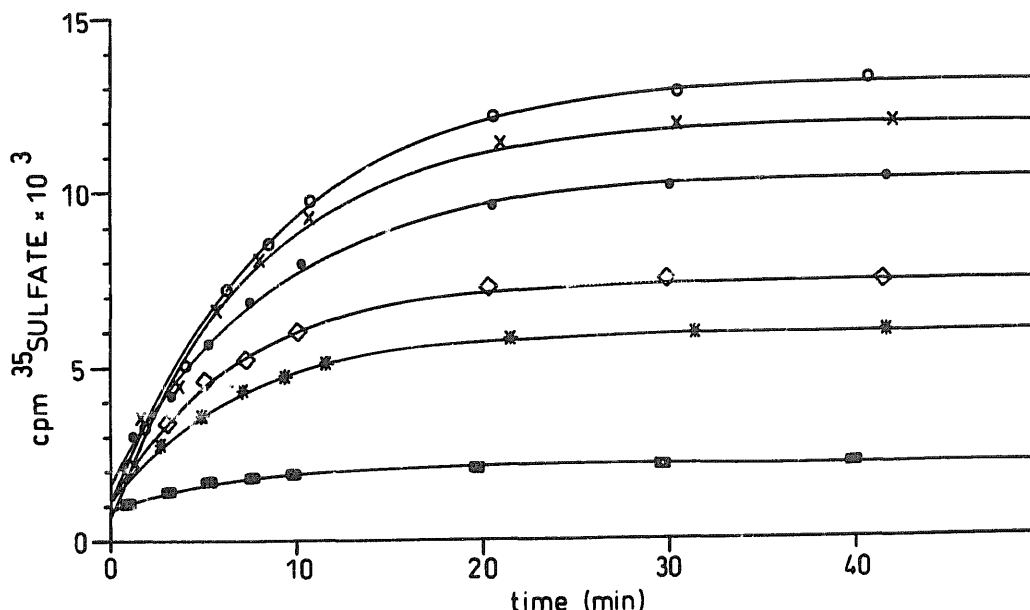


Fig. 2. Survival of human red cell ghosts at  $60^\circ\text{C}$ . The lines drawn represent single exponentials fitted to the time-course of appearance of  $^{35}\text{SO}_4^{2-}$  in the supernatant at  $37^\circ\text{C}$  as measured after preincubation at  $60^\circ\text{C}$  for the following lengths of time:  $\circ$ , no preincubation at  $60^\circ\text{C}$ ;  $\times$ , 7.5 min;  $\bullet$ , 15 min;  $\diamond$ , 30 min;  $*$ , 45 min;  $\blacksquare$ , 90 min. The flux medium comprised 130 mM NaCl/1 mM  $\text{Na}_2\text{SO}_4$ /20 mM EDTA (pH 6.5). The rate constants are listed in Table I.

TABLE I

EFFECT OF PREINCUBATION AT 60°C FOR VARIOUS LENGTHS OF TIME ON SULFATE EQUILIBRIUM EXCHANGE AS MEASURED AT 37°C

The percentage of leaky ghosts was calculated from the retention of  $^{35}\text{SO}_4^{2-}$  in the ghosts at the end of the preincubation period at 60°C. Retention was measured after three washes in the nonradioactive chloride medium (130 mM NaCl/1 mM  $\text{Na}_2\text{SO}_4$ /20 mM EDTA (pH 6.5)) at 0°C.

Experimental condition: Time of preincubation at 60°C (min)	no $\text{H}_2\text{DIDS}$ present		$\text{H}_2\text{DIDS}$ present		$\text{H}_2\text{DIDS}$ sensitive
	leaky ghosts (%)	$^{\circ}k_s$ ( $\text{min}^{-1}$ )	leaky ghosts (%)	$^{\circ}k_s \cdot 10^3$ ( $\text{min}^{-1}$ )	$^{\circ}k_s$ ( $\text{min}^{-1}$ )
0	0	0.121	0	3.68	0.118
7.5	10.6	0.123	0	2.71	0.120
15	23.3	0.115	1.8	3.96	0.111
30	45.1	0.140	14.3	7.19	0.133
45	59.9	0.157	28.4	11.5	0.145
90	85.1	0.165	76.3	26.4	0.137

leakiness significantly influences the measurements.

*Temperature dependence of sulfate equilibrium exchange between 20 and 60°C*

The temperature dependence of sulfate equilibrium exchange was measured in media containing 108 mM  $\text{Na}_2\text{SO}_4$  and no chloride, or 1.0 mM  $\text{Na}_2\text{SO}_4$ /130 mM NaCl. In both cases, 20 mM EDTA (pH 6.5) served as a buffer.

Fig. 3 summarizes the results. They confirm that over the temperature range 15–30°C, the

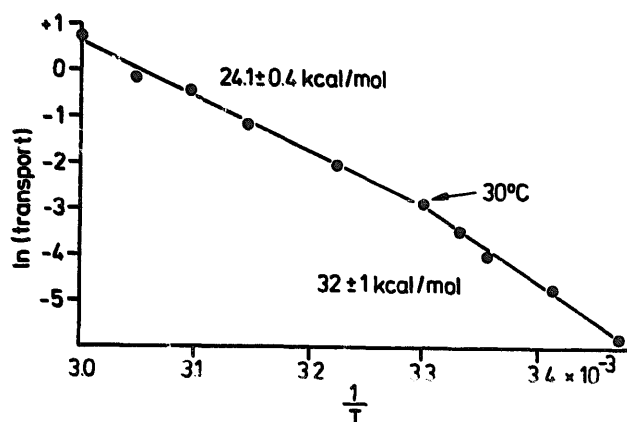


Fig. 3. Arrhenius plot of the temperature dependence of sulfate efflux from human red cell ghosts in chloride medium. The term transport on the ordinate refers to the rate constants corrected for non-band-3-mediated sulfate efflux by subtracting the rate constants of the  $\text{H}_2\text{DIDS}$ -treated controls. The activation energies ( $E_a$ ) indicated in the figure were calculated from the slopes of the straight lines above and below 30°C.

activation energy is 32 kcal/mol. This result is obtained regardless of whether the measurements were made in the presence of  $\text{Cl}^-$  or  $\text{SO}_4^{2-}$  as the predominant anion species (Table II). Over the temperature range 30–60°C, the calculated activation energy is 24.1 kcal/mol. Again, a similar result was obtained when the measurements were performed in sulfate medium (Table II). Thus the Arrhenius curve shows an inflection somewhere between 30 and 37°C.

*Temperature dependence of  $\text{Cl}^-$  binding and  $\text{Cl}^-$  /  $\text{SO}_4^{2-}$  competition at the band 3 protein*

It has been shown by Chan and associates [3] that  $\text{Cl}^-$  binding to the band 3 protein can be determined by measuring the change of line broadening induced by replacement of  $\text{Cl}^-$  from the band 3 protein by the addition of a large

TABLE II

ACTIVATION ENERGIES ( $E_a$ ) FOR SULFATE EQUILIBRIUM EXCHANGE ABOVE AND BELOW 37°C IN CHLORIDE AND SULFATE MEDIUM

Medium	Temperature range (°C)	$E_a$ (kcal/mol)	$\pm \sigma_M$	$n$
$\text{SO}_4^{2-}$	37–60	23.5	1.5	4
	37–20	31.7	0.8	3
$\text{Cl}^-$	37–60	24.1	0.4	3
	37–20	32.6	0.8	15
	37–18			

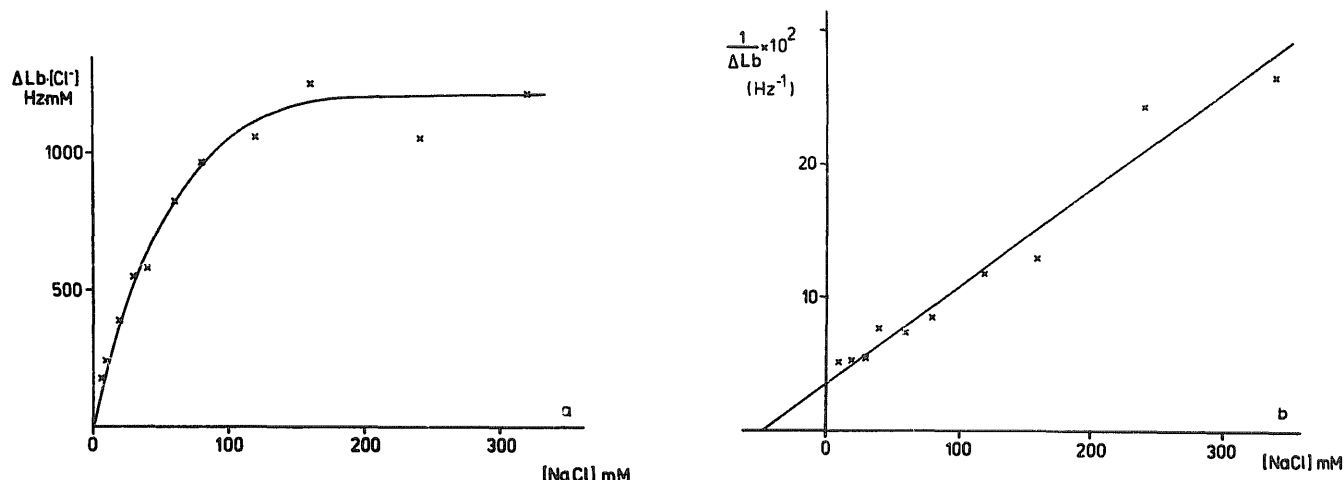


Fig. 4. (a)  $\text{Cl}^-$ -binding to the band 3 protein in resealed red cell ghosts at  $26^\circ\text{C}$ . The ghosts had been resealed in media containing 20 mM EDTA with the NaCl concentrations indicated on the abscissa (pH 7.4). Ordinate: change of line width caused by the addition of a large excess of DNDS. The solid line has been calculated using a half-saturation constant of 45 mM. (b) Reciprocal plot of the data from (a). Half-saturation constant 45 mM.

excess of the anion transport inhibitor DNDS. In accordance with the previous work of the authors mentioned, we find that, at  $26^\circ\text{C}$ , the DNDS-replaceable  $\text{Cl}^-$ -binding follows a saturation curve with half-saturation at 40–60 mM (Figs. 4a, 4b). Essentially similar values are obtained over the whole temperature range of  $3\text{--}42^\circ\text{C}$  (Table III). This indicates that the temperature coefficient of  $\text{Cl}^-$  binding to band 3 is negligibly small.

To extend the range of measurements without being compelled to determine  $K_{1/2}$  values, we prepared red cell ghosts in media containing 30 and 45 mM NaCl. These concentrations are below or close to the  $K_{1/2}$  value found above and hence within the nearly linear portion of the saturation

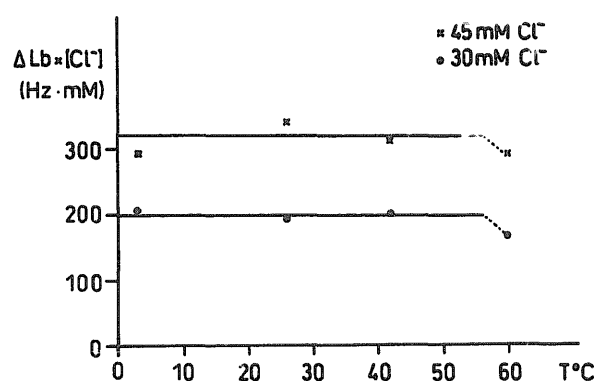


Fig. 5. DNDS-sensitive chloride-binding as a function of temperature. Composition of the media: 20 mM EDTA and either 45 mM  $\text{Cl}^-$  (x) or 30 mM  $\text{Cl}^-$  (o) (pH 6.5). For data at  $60^\circ\text{C}$  and higher, see Figs. 6 and 7.

TABLE III

HALF-SATURATION CONCENTRATIONS ( $K_{1/2}$ ) FOR BAND-3-MEDIATED CHLORIDE TRANSPORT AND CHLORIDE-BINDING TO BAND 3

Data for chloride transport from Brahm [2]. Data for chloride binding refer to DNDS-sensitive chloride-binding as determined by NMR.

Chloride transport		Chloride binding	
temperature ( $^\circ\text{C}$ )	$K_{1/2}$ (mmol/l)	temperature ( $^\circ$ )	$K_{1/2} \pm \text{S.D.}$ (mmol/l)
0	28	0	$60 \pm 9$
10	35	10	$61 \pm 23$
25	47	25	$32 \pm 10$
38	65	42	$49 \pm 11$

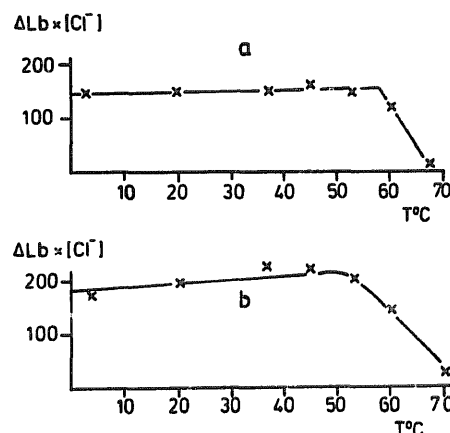


Fig. 6. DNDS-sensitive  $\text{Cl}^-$ -binding as a function of temperature. Composition of the media: (a) 20 mM EDTA/30 mM NaCl/1 mM  $\text{Na}_2\text{SO}_4$  (pH 7.4); (b) 20 mM EDTA/30 mM NaCl/40 mM  $\text{Na}_2\text{SO}_4$  (pH 7.4).

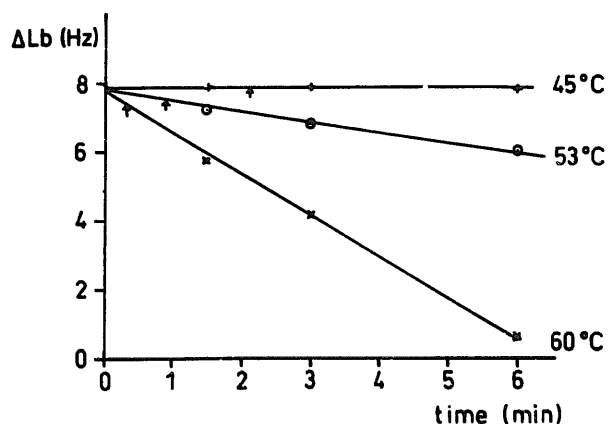


Fig. 7. Changes of the  $\text{Cl}^-$ -binding to the band 3 protein at 45, 53 and 60 °C. The arrows show the bound  $\text{Cl}^-$  after the time  $0.69/^\circ\text{k}_s$ , where  $^\circ\text{k}_s$  represents the rate constants for  $\text{SO}_4^{2-}$  equilibrium exchange. Ordinate: change of the linewidth upon replacement of bound  $^{35}\text{Cl}$  by a large excess of DNDS. Composition of the medium: 30 mM NaCl/1 mM  $\text{Na}_2\text{SO}_4$ /20 mM EDTA (pH 6.5).

curve. Under this condition, any change of binding due to changes of temperature should be easily measurable by determination of the  $\text{Cl}^-$  that can be displaced by a large excess of DNDS. No change could be discovered up to nearly 60 °C (Fig. 5). Above this temperature, binding abruptly decreases (Fig. 6). The decrease of  $\text{Cl}^-$ -binding capacity is a function of the time required for the flux measurements. At 60 °C this decrease begins immediately and continues to nearly zero within about 6 min (Fig. 7). However, for this and all other temperatures below 60 °C, the decrease of  $\text{Cl}^-$ -binding caused by heat denaturation of band 3 is slow compared to the rate of  $^{35}\text{SO}_4$  exchange. If one takes readings of  $\Delta\text{Lb}$  from the curves in Fig. 7 at the times corresponding to the time constants of sulfate equilibrium exchange, as measured at the same temperatures, one obtains values that are virtually independent of temperature and indistinguishable from the readings at temperatures below 45 °C, where  $\Delta\text{Lb}$  does not change with temperature.

In another set of experiments, red cell ghosts were equilibrated in a medium containing 40 mM  $\text{Na}_2\text{SO}_4$  in addition to 30 mM NaCl. Since  $\text{Cl}^-$  and  $\text{SO}_4^{2-}$  are known to compete for the same site on band 3, temperature-dependent changes of  $\text{SO}_4^{2-}$  binding should lead to changes of  $\text{Cl}^-$ -binding. The changes observed over the temperature

range 3–60 °C are represented in Fig. 6. The figure shows that the temperature coefficient for  $\text{SO}_4^{2-}$ -binding to the common binding site for  $\text{Cl}^-$  and  $\text{SO}_4^{2-}$  is as small as that for  $\text{Cl}^-$ -binding, i.e., negligibly small.

## Discussion

The sulfate efflux at 60 °C consists of rapid band-3-mediated transport and a much slower penetration across leaks. The transport is completed within about 1 min (Fig. 1), while the efflux across the leaks takes place at a rate of about 1.5% per min (see Table I). When the ghosts are made from red cells with covalently bound  $\text{H}_2\text{DIDS}$ , the rate of leakage is considerably reduced for the first 5 or 10 min of incubation at 60 °C (Table I). This suggests that, at least during this time interval, the exposure to the elevated temperature does not induce generalized damage of the permeability barrier. Instead, the initial  $\text{SO}_4^{2-}$  leakage seems to proceed largely via the heat-denatured band 3 protein. This inference is supported by NMR measurements. These show that the capacity of the band 3 protein for anion binding is lost during incubation at the elevated temperature, but that this loss occurs much more slowly than the band-3-mediated  $\text{SO}_4^{2-}$  equilibration across the membrane. If one proceeds to temperatures above 60 °C, the rate of denaturation of band 3 seems to be augmented to a higher degree than is the rate of band-3-mediated transport. Thus, the band 3 protein and the permeability barrier of the red cell ghosts survive up to 60 °C for a length of time that suffices for the execution of transport studies with  $^{35}\text{SO}_4^{2-}$ .

This made it possible to demonstrate that the activation energy decreases from 32 kcal/mol as measured over the range 20–37 °C, to 24.1 kcal/mol in the range 37–60 °C. Thus, the occurrence of a break in the Arrhenius plot is not confined to the halides. It has nothing to do with the valency of the transported anion and seems to represent a general feature of band-3-protein-mediated anion transport. According to Brahm [2], the turnover numbers of  $\text{Cl}^-$  and  $\text{Br}^-$  are about equal at the respective temperatures at which the Arrhenius plots show the breaks ( $4 \cdot 10^3$  ions/band 3 per s.) For sulfate, at 60 °C, the



turnover number is 240 ions/band 3 per s and hence still at least one order of magnitude below the value inferred from the work with halides. The concept of a critical turnover number is, therefore, no longer tenable when anions other than the halides are included in the picture. Below, the temperature dependence of anion transport will be discussed in terms of ping-pong kinetics, which have proven to be fruitful for the description of band 3 protein-mediated anion transport (for reviews, see Refs. 1, 6 and 7). The discussion will be organized as follows:

(1) The equations for ping-pong kinetics at equilibrium will be presented. The effects of the various temperature-dependent parameters defined by ping-pong kinetics on the overall temperature dependence will be described, and those parameter values will be identified that are most likely to determine the actually observed temperature-dependence.

(2) The thermodynamic quantities defined by the theory of absolute reaction rates ( $\Delta G^\ddagger$ ,  $\Delta H^\ddagger$ ,  $\Delta S^\ddagger$ ) will be calculated for the rate-limiting parameters and their significance for the molecular mechanism of band-3-mediated anion transport will be discussed.

#### *Equations for ping-pong kinetics at equilibrium exchange*

The band 3 protein exists in the red blood cell membrane in at least two different conformations

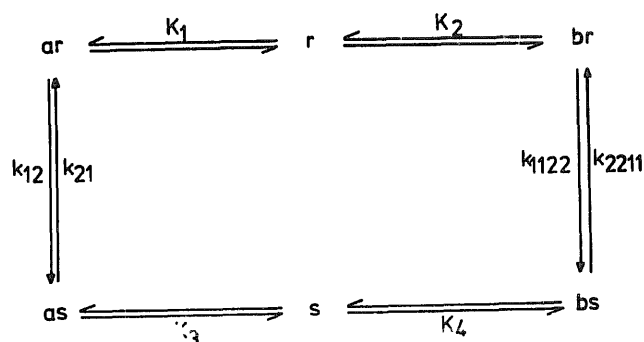


Fig. 8. Ping-pong kinetics of anion transport. The figure serves to define the various rate constants and mass law constants used in the mathematical derivations.  $K_1$ ,  $K_2$ ,  $K_3$ ,  $K_4$  are mass law constants.  $k_{12}$ ,  $k_{21}$ ,  $k_{1122}$ ,  $k_{2211}$  are rate constants.  $a$ ,  $b$  refer to chloride and sulfate, respectively.  $r$  and  $ar$  or  $br$  indicate unloaded and anion-loaded band 3 molecules facing inward.  $s$  and  $as$  or  $bs$  indicate unloaded and anion-loaded band 3 molecules facing outward.

(Fig. 8). In one conformation, the substrate binding site faces outward, in the other conformation inward. In the absence of anions that are accepted by the protein as a substrate, the transition from one to the other conformation is a slow process which cannot be measured by the currently existing methods. There is no 'slippage'. When a substrate anion becomes bound, the energy barriers which impede the transitions are reduced and a rapid equilibration takes place. The anion catalyzes the conformational changes. In the course of this catalytic process, the anion is moved across the membrane. This mechanism gives rise to ping-pong kinetics.

If sulfate competes with chloride for a common transport site, ping-pong kinetics lead to the following expression (Ref. 1, Fig. 8):

$$J_b = \frac{k_{1122} \cdot k_{2211} \cdot \overline{RS} \cdot b}{k_{2211}U + K_{1122}V} \quad (1)$$

where

$$U = b + K_2 \left( 1 + \frac{a}{K_1} \right) \quad (1a)$$

and

$$V = b + K_4 \left( 1 + \frac{a}{K_3} \right) \quad (1b)$$

$a$  and  $b$  refer to the concentrations of chloride and sulfate, respectively; the remaining symbols refer to the rate constants ( $k$ ) and mass law constants ( $K$ ) defined by the reaction diagram in Fig. 8.  $\overline{RS} = r + ar + s + as$ .

In sulfate medium with no  $\text{Cl}^-$  present ( $a = 0$ ),

$$U = K_2 + b \quad (1c)$$

and

$$V = K_4 + b \quad (1d)$$

In chloride medium, with only little  $\text{SO}_4^{2-}$  present, the transporter is far from saturation with sulfate (i.e.,  $b \ll K_2$ ,  $K_4$ ) and near saturation with respect to chloride

$$U = a \cdot K_2 / K_1 \quad (1e)$$

and

$$V = a \cdot K_4 / K_3 \quad (1f)$$

For  $\text{Cl}^-$  at  $0^\circ\text{C}$ , it has been shown that the mass law constants for combination with the inward-directed (r) and outward-directed (s) transfer site are virtually equal (i.e.,  $K_1 = K_3 = K_a$ ) [6]. If we assume that this is true at all temperatures between  $0^\circ$  and  $60^\circ\text{C}$ , and also applies to sulfate (i.e.  $K_2 = K_4 = K_b$ ) then

$$U = V = b + K_b(1 + a/K_a)$$

and

$$J_b = \frac{k_{1122} \cdot k_{2211}}{k_{2211} + k_{1122}} \frac{\overline{RS}}{b + K_b(1 + a/K_a)} \quad (2)$$

In principle, the rate constants  $k_{1122}$  and  $k_{2211}$ , as well as the terms  $U$  and  $V$  in Eqn. 1 could vary with temperature. Hence, in terms of the simplified expression Eqn. 2, both

$$j_{\max} = \frac{k_{1122} \cdot k_{2211}}{k_{2211} + k_{1122}} \overline{RS} \quad \text{and} \quad K_{1/2} = K_b \left(1 + \frac{a}{K_a}\right)$$

could be temperature dependent.

#### Temperature dependence of $j_{\max}$

Assuming

$$k_{1122} = k_{1122}^0 \exp\left(-\frac{E_{1122}}{RT}\right) \quad \text{and} \quad k_{2211} = k_{2211}^0 \exp\left(-\frac{E_{2211}}{RT}\right)$$

(see Ref. 1), one obtains:

$$j_{\max} = \frac{k_{1122}^0 \cdot k_{2211}^0 \cdot \overline{RS}}{k_{2211}^0 \exp\left(+\frac{E_{1122}}{RT}\right) + k_{1122}^0 \exp\left(+\frac{E_{2211}}{RT}\right)} \quad (3)$$

$k_{1122}^0$  and  $k_{2211}^0$  are temperature-independent rate coefficients, and  $E_{1122}$  and  $E_{2211}$  the corresponding Arrhenius activation energies.  $R$  and  $T$  have their usual meanings.

According to Eqn. 1 or Eqn. 2, for  $k_{1122} \ll k_{2211}$  the temperature-dependence is dominated by  $k_{1122}$ ; for  $k_{2211} \ll k_{1122}$  it is dominated by  $k_{2211}$ . Under these two limiting conditions an Arrhenius plot (i.e., a plot of  $\ln j$  vs.  $1/T$ ) yields straight lines with the slopes  $E_{1122}$  and  $E_{2211}$ , respectively. One

now needs to determine which of the experimentally observed activation energies pertains to  $k_{1122}$  or to  $k_{2211}$ . In our specific case this can be done using the relationship

$$\frac{k_{1122}}{k_{2211}} \cdot \frac{K_1 \cdot K_4}{K_2 \cdot K_3} = \frac{k_{12}}{k_{21}} \quad (\text{see Fig. 8})$$

It has already been pointed out above that, most likely,  $K_1 = K_3$  and  $K_2 = K_4$ . Hence this expression leads to

$$k_{1122}/k_{2211} = k_{12}/k_{21}.$$

It is known that at  $0^\circ\text{C}$ ,  $k_{12}/k_{21} \ll 1.0$ . We may conclude, therefore, that this is also true for  $k_{1122}/k_{2211}$ . Since  $k_{12}/k_{21} = as/ar$  and  $k_{1122}/k_{2211} = bs/br$ , this means that the number of inward-oriented, substrate-loaded transport protein molecules exceeds the number of outward-oriented molecules. Hence the constant activation energy measured between  $0^\circ\text{C}$  and the break in the Arrhenius plot should correspond to  $E_{1122}$  and pertain to the rate of conformational transition  $br \rightarrow bs$ .

#### Temperature dependence of $k_{1/2}$

Temperature-dependent changes of the mass law constants for the binding of the substrates a and/or b (i.e.,  $K_1$ ,  $K_2$ ,  $K_3$ ,  $K_4$  in Eqn. 1 or  $K_a$  and  $K_b$  in Eqn. 2) could contribute to the temperature dependence of the flux  $j_b$ . Such contributions would be absent only if either (i) the substrate concentrations are sufficiently high to ensure complete saturation of the transport system at all temperatures at which the flux measurements are performed or (ii) the affinities for  $\text{Cl}^-$  and  $\text{SO}_4^{2-}$ -binding remain constant at all temperatures covered.

Assumption (i) is reasonably justified if one accepts the published apparent  $K_m$  values for  $\text{Cl}^-$  (20–65 mmol/l) and  $\text{SO}_4^{2-}$  (about 40 mmol/l) derived from studies of the concentration dependence of  $\text{Cl}^-$  (Brahm, Ref. 2) and  $\text{SO}_4^{2-}$  (Gunn, Ref. 7) flux, respectively (reviewed in Ref. 1). NMR measurements of  $\text{Cl}^-$ -binding and  $\text{Cl}^-/\text{SO}_4^{2-}$  competition yielded results which suggest that the mass law constants for binding of  $\text{Cl}^-$  to band 3 are of the order predicted by

kinetics, while the constants for  $\text{SO}_4^{2-}$ -binding are 3–4-times higher (unpublished results), yielding  $K_m$  values of 120–140 mmol/l. The kinetic studies suffer certain shortcomings. The kinetics are complicated by self-inhibition of anion exchange at more elevated concentrations, which tends to simulate saturation even though the transport sites may still be far from being completely occupied. As a consequence, the half-saturation constants could be underestimated. This problem does not exist for the NMR measurements, since the substrate binding to the transport site is measured independently of substrate binding to other sites on the band 3 protein.

Our determinations of the half-saturation constant for  $\text{Cl}^-$ -binding to the band 3 protein by means of the NMR technique yielded values of between 40–60 mmol/l, with no measurable temperature dependence over the range 0–42°C. Over the more elevated temperature range up to 60°C, we confined ourselves to demonstrating the absence of an effect of temperature on  $\text{Cl}^-$ -binding and  $\text{Cl}^-/\text{SO}_4^{2-}$  competition at two selected  $\text{Cl}^-$  concentrations (below or at  $K_{1/2}$ , where the sensitivity towards the effects of temperature is maximal), or at one fixed  $\text{Cl}^-/\text{SO}_4^{2-}$  ratio. In both instances, effects of temperature were small or absent, indicating that, up to 60°C, neither the binding of  $\text{Cl}^-$  nor that of  $\text{SO}_4^{2-}$  contributes enthalpy changes that significantly affect the Arrhenius activation energies.

This conclusion is in accordance with determinations of the apparent Michaelis constants for  $\text{SO}_4^{2-}$  transport at temperatures between 25 and 37°C. These determinations revealed only slight changes, which suggest that the enthalpy changes associated with anion binding are small, maximally of the order of 2–3 kcal/mol [8].

#### *Interpretation of the data in terms of the theory of absolute reaction rates*

According to the theory of absolute reaction rates, the rate-limiting transport step is preceded by an activation process which is characterized by the free enthalpy of activation ( $G^\ddagger$ ). According to Eyring [9], one may write

$$k_t = \kappa \frac{RT}{N_L h} \exp\left(-\frac{\Delta G^\ddagger}{RT}\right)$$

where

$$\Delta G^\ddagger = \Delta H^\ddagger - T\Delta S^\ddagger$$

In these expressions,  $k_t$  represents the turnover number of the loaded transport protein, in ions/band 3 per s.  $\Delta H^\ddagger$  and  $\Delta S^\ddagger$  indicate, respectively, the changes of enthalpy and entropy associated with the activation process. The factor  $\kappa$  refers to the fraction of molecules in the transition state that continue with the reaction to completion (transmission coefficient). We assume  $\kappa = 1$ .

Table IV contains a compilation of the thermodynamic parameters as defined by the theory of absolute reaction rates. For all anion species listed, the large activation enthalpy below the break is largely compensated by a large activation entropy. This is the reason why, in spite of the existence of large energy barriers, the turnover numbers of anion transport (notably of halide transport) are high.

Below the break, the  $\Delta H^\ddagger$  values for the three species of anion studied are similar, amounting to 30–35 kcal/mol. Above the break, they assume values between 19.2 and 24 kcal/mol. Most dramatic is the reduction, of activation entropy from values of 61–41 cal/mol per K to values of 27–20 cal/mol per K. As a net result of the

TABLE IV

THERMODYNAMICS OF THE ACTIVATION PROCESS ASSOCIATED WITH BAND 3-MEDIATED TRANSPORT OF  $\text{Cl}^-$ ,  $\text{Br}^-$  AND  $\text{SO}_4^{2-}$

Turnover number: ions · (band 3 · s)<sup>-1</sup>;  $\Delta G^\ddagger$ ,  $\Delta H^\ddagger$ ,  $T\Delta S^\ddagger$  in cal/mol.  $\Delta S^\ddagger$  in cal/mol per K.  $\text{Cl}^-$  and  $\text{Br}^-$  transport measured at 150 mM  $\text{Cl}^-$  or  $\text{Br}^-$  in the medium, respectively (pH 7.2).  $\text{SO}_4^{2-}$  transport at 108 mM  $\text{SO}_4^{2-}$  in the medium (pH 6.5). The calculation of the thermodynamic parameters for  $\text{Cl}^-$  and  $\text{Br}^-$  are based on the data of Brahm [2].

Temp. (°C)	Anion species	Turnover number	$\Delta G^\ddagger$	$\Delta H^\ddagger$	$T\Delta S^\ddagger$	$\Delta S^\ddagger$
0	$\text{Cl}^-$	234	13000	27600	14600	+53.5
38	$\text{Cl}^-$	42646	11600	18800	7100	+23.0
0	$\text{Br}^-$	25.8	14000	31000	16800	+61.5
38	$\text{Br}^-$	15226	12300	20700	8400	+27.0
20	$\text{SO}_4^{2-}$	1.1	17100	29000	11900	+41.0
60	$\text{SO}_4^{2-}$	240.3	16000	22600	6700	+20.0

changes of both  $\Delta H^\ddagger$  and  $\Delta S^\ddagger$ , the free enthalpy of activation of the various anion species studied changes by no more than 10–30%.

From the data and the calculations one important conclusion can be drawn concerning the mechanism of the band-3-mediated anion transport: the partial compensation of the activation enthalpy by the large entropy suggests that the activation process involves major changes of water structure and/or of the structure of the transport protein, possibly including regions of the peptide chain far distant from the substrate-binding site.

This conclusion is entirely in keeping with measurements of the activation volume which yielded the enormous value of about 150 ml/mol (as compared to  $-30$  to  $+30$  ml in ordinary enzymatic reactions) [10]. It agrees well with observations of transport-related allosterical interactions between amino-acid residues of the band 3 molecule at locations far distant from one another (see Table IV in Ref. 1, which lists a large number of these interactions, including interactions between amino-acid residues located at opposite surfaces of the membrane). Thus the band 3 protein seems to be specifically adapted to execute its transport function by undergoing major structural changes that involves large segments of the peptide chain, rather than localized changes that are confined to the oscillations of a few amino-acid residues at a narrow anion gate. If such localized changes were important, they would be affected by changes in many other regions of the large transport molecule.

#### *Interpretation of the break in the Arrhenius plot: a hypothesis*

In chemical kinetics, changes of Arrhenius activation energy with temperature are not infrequent. They indicate a change of a rate-limiting step. In membrane transport processes, one should consider the possibility that this is the consequence of a phase transition in the lipid bilayer. In our case, this does not seem to apply, since the temperatures at which these changes occur are different from the three different anion species studied. Moreover, measurements of  $\text{SO}_4^{2-}$  transport in  $\text{SO}_4^{2-}$  medium or  $\text{Cl}^-$  medium yield the same result, indicating that the differences of the

ionic composition of the media in which  $\text{Cl}^-$  and  $\text{SO}_4^{2-}$  transport had been measured, make no difference. We feel compelled, therefore, to look for some other explanation.

The interpretation of anion exchange in terms of ping-pong kinetics includes the assumption that the overall transport reaction depends on the rate constants for the transitions of the substrate-loaded transport protein from one surface to the other and vice versa. If the relative magnitudes of the two constants vary with temperature, then one can expect to observe in the Arrhenius plots two regions with different slopes, depending on which of the two rates is rate-limiting. For example, if the rate constant  $k_{1122}$  for the transition from inside to outside has a higher temperature coefficient than the rate constant for the transition in the reverse direction, then one would expect a limiting slope corresponding to the activation energy  $E_{1122}$  at low temperatures, and a limiting slope corresponding to the activation energy  $E_{2211}$  at high temperatures (see Eqn. 3). It seems instructive to consider the consequences that follow from this simple assumption and to compare them with experimental observations available in the literature.

According to the theory of absolute reaction rates, the conformational changes of the substrate-loaded transport protein pass through transition states:



For the reaction from inside to outside ( $\text{br}^\ddagger \rightarrow \text{bs}$ ), we may write (assuming that the transmission coefficient is equal to 1.0):

$$k_{1122} = \frac{RT}{N_A \cdot h} \cdot K'$$

and for the reaction in the opposite direction

$$k_{2211} = \frac{RT}{N_A \cdot h} \cdot K''$$

$K'$  and  $K''$  represent pseudo-equilibrium constants between the reactants and their respective transition states,  $\text{br}^\ddagger$  and  $\text{bs}^\ddagger$ . Thus:

$$\frac{k_{1122}}{k_{2211}} = \frac{\text{bs}}{\text{br}} = \frac{K'}{K''} = K_{\text{eq}}$$

Applying standard thermodynamics one may write:

$$RT \ln K' = \Delta G^{\#'} = \Delta H^{\#'} - T\Delta S^{\#'}$$

$$RT \ln K'' = \Delta G^{\#''} = \Delta H^{\#''} - T\Delta S^{\#''}$$

and for the difference

$$\Delta G^{\#'} - \Delta G^{\#''} = \Delta H^{\#'} - \Delta H^{\#''} - T(\Delta S^{\#'} - \Delta S^{\#''}) \quad (4)$$

The differences  $\Delta G^{\#'} - \Delta G^{\#''}$ ,  $\Delta H^{\#'} - \Delta H^{\#''}$  and  $\Delta S^{\#'} - \Delta S^{\#''}$  represent, respectively, the changes of free enthalpy, enthalpy and entropy of the overall reaction  $bs/br = K_{eq}$ . The symbol # indicates that all quantities refer to the pseudo-equilibrium between the reactants and their transition states, and the symbols ' and '' indicate the reactions  $br \rightleftharpoons br^{\#}$  and  $bs \rightleftharpoons bs^{\#}$ , respectively. Equations analogous to those derived above for anion species b also apply to anion species a where

$$\frac{k_{12}}{k_{21}} = \frac{as}{ar}$$

We now introduce the assumption that the activation enthalpies and entropies calculated for the temperature range above the break in the

Arrhenius plots refer to  $k_{2211}$ , and below the break to  $k_{1122}$ . If we further assume that these quantities are independent of temperature, we may use Eqn. 4 to calculate the thermodynamic parameters for the overall reaction  $bs/br = K_{eq}$  (Table V) as a function of temperature. The data on  $Cl^-$  transport are particularly interesting, since they lead to a prediction that can be checked against available experimental evidence. At  $0^\circ C$ , our calculations predict that the equilibrium  $ar \rightleftharpoons as$  favors  $ar$ , i.e., the inward-oriented conformer. Studies on the recruitment of band 3 under the influence of ionic gradients yielded (at  $0^\circ C$ ) values of  $k_{12}/k_{21} = 0.05$  [12] or 0.3–0.4 [13] (reviewed in Ref. 1), which should be compared with the present value (Table V) of about 0.4. Our data suggest, therefore, that the analysis presented here is worth pursuing in future work.

## Appendix

The derivation of Eqn. 1 is based on the following assumptions:

(1) Mass law:

$$\text{at surface '' : } a'' \cdot r/ar = K_1; b'' \cdot r/br = K_2$$

$$\text{at surface ' : } a' \cdot s/as = K_3; b' \cdot s/bs = K_4$$

between surfaces ' and '':

$$ar/as = k_{21}/k_{12};$$

$$br/bs = k_{2211}/k_{1122}$$

(2) Steady state:

$$k_{12}ar + k_{1122}br = k_{21}as + k_{2211}bs$$

(3) Mass balance:

$$ar + r + as + s = \overline{RS}$$

Note: if  $a' = a''$  and  $b' = b''$  then the equations listed under (1) and (2) yield:

$$K_1 K_4 / K_2 K_3 = (k_{12}/k_{21}) \cdot (k_{2211}/k_{1122})$$

Combination of all the equations listed above, assuming  $a' = a''$ ,  $b' = b''$ , and taking this expression into account leads to Eqn. 1 in the text.

TABLE V

THERMODYNAMICAL PARAMETERS FOR THE DISTRIBUTION EQUILIBRIUM BETWEEN INWARD-ORIENTED AND OUTWARD-ORIENTED SUBSTRATE-LOADED CONFORMERS OF THE BAND 3 PROTEIN

Values calculated from the data in Table IV as described in the text. Values of  $K_{eq} < 1.0$  indicate a preferential orientation of the substrate-loaded transport protein to the inside;  $K > 1.0$  indicates preferred orientation in the opposite direction. The calculations are based on hypothetical assumptions.

Temp. (°C)	$\Delta G$ (cal/mol)	$\Delta H$ (cal/mol)	$\Delta S$ (cal/mol per K)	$K_{eq}$	Anion species
0	-456.5	8780	30.5	0.43	$Cl^-$
38	-702.5	8780	30.5	3.12	$Cl^-$
0	+861.2	10280	34.5	0.20	$Br^-$
38	-449.0	10280	34.5	2.10	$Br^-$
20	+353.0	6420	20.7	0.55	$SO_4^{2-}$
60	-475.4	6420	20.7	2.05	$SO_4^{2-}$

## Acknowledgements

We thank Mrs. B. Legrum and E. Gärtner for their support and Drs. D. Schubert, W. Schwarz and Ph. Wood for reading the manuscript and their valuable comments.

## References

- 1 Passow, H. (1986) *Rev. Physiol. Biochem. Pharmacol.* 103, 61–223.
- 2 Brahm, J. (1977) *J. Gen. Physiol.* 70, 283–306.
- 3 Falke, J.F., Pace, R.J. and Chan, S.I. (1984) *J. Biol. Chem.* 259, 6472–6480.
- 4 Schwoch, G. and Passow, H. (1973) *Mol. Cell. Biochem.* 2, 197–218.
- 5 Ku, C.P., Jennings, M.L. and Passow, H. (1979) *Biochim. Biophys. Acta* 553, 132–144.
- 6 Knauf, Ph. (1986) in *Membrane Transport Disorders* (Andreoli, T., Hoffman, J.F., Schultz, S.G. and Fanenstil, D.D., eds.) 2nd ed. pp. 191–220, Plenum, New York.
- 7 Gunn, R.B. and Fröhlich, O. (1986) *Biochim. Biophys. Acta* 864, 169–194.
- 8 Gunn, R.B. (1978) in *Membrane Transport Processes* (Hoffman, J.F., ed.) Vol. 1, pp. 61–77, Raven, New York.
- 9 Gardour, R.D. and Schowen, R.L. (eds.) (1978) *Transition States of Biochemical Processes*, Plenum, New York.
- 10 Canfield, V.A. and Macey, R.I. (1984) *Biochim. Biophys. Acta* 778, 379–384.
- 11 Gershfeld, N.L. and Murayama, M. (1988) *J. Membr. Biol.* 101: 67–72.
- 12 Gunn, R.B. and Fröhlich, O. (1979) *J. Gen. Physiol.* 74, 351–374.
- 13 Hautmann, M. and Schnell, K.F. (1985) *Pflügers Arch.* 405, 193–201.